Available online at www.sciencedirect.com
ScienceDirect
Polymer 48 (2007) 5133–5145
polymer
www.elsevier.com/locate/polymer

Morphology and shape memory effect of segmented polyurethanes. Part I: With crystalline reversible phase

Feng Long Ji [a], Jin Lian Hu [a,*], Ting Cheng Li [b], Yuen Wah Wong [c]

[a] *Institute of Textile and Clothing, Hong Kong Polytechnic University, Kowloon, Hong Kong, PR China*
[b] *Institute of Advanced Materials, Fudan University, 220 Handan Road, Shanghai 200433, PR China*
[c] *Department of applied physics, Hong Kong Polytechnic University, Hong Kong, PR China*

Received 15 November 2006; received in revised form 12 June 2007; accepted 15 June 2007
Available online 22 June 2007

Abstract

A set of segment polyurethanes were synthesized and were proved to have interconnected, isolated and no hard-segmented domains. It was found that the shape fixity of the polyurethanes decreased with the increase of hard-segment content. The polyurethanes with hard-segment content from 30% to 50% had to be deformed at least to 100% strain to obtain good shape fixity. The segmented polyurethane having no hard-segment domains showed over 90% shape recovery under particular conditions. The segmented polyurethanes having interconnected hard-segment domains showed dramatically decreased shape recovery. The segmented polyurethanes having isolated hard-segment domains showed better shape recovery. When the polyurethanes were heated up to sufficiently high temperature they mostly recovered to their original shape. Stress relaxation would bring decrease to the shape recovery of the polyurethanes, especially to that of the segmented polyurethanes with low hard-segment content of 15% and 20%. For the segmented polyurethanes have isolated hard-segment domains the shape recovery decreased when the deformation amplitude increased from 50% to 200% and stopped decreasing as deformation amplitude increased to 250%. The shape recovery of the segmented polyurethanes could be enhanced nearly to 100% by a pre-deformation treatment.

Keywords: Shape memory; Polyurethane; Small angle X-ray scattering

1. Introduction

As a class of novel smart materials, shape memory polymers (SMPs) can deform enormously above a transition temperature (T_{trans}) and can mostly be fixed in a temporary shape by cooling below T_{trans}. After reheating above T_{trans}, they can automatically recover to their original shape. SMPs have attracted extensive attention and are considered to be promising for many applications including actuators, sensors [1], biomaterials [2], and smart textiles [3].

The polymers designed to exhibit good shape memory effect including shape recovery and shape fixity, were intrinsically polymer networks [4–18]. The network chains showing a thermal transition at T_{trans} play a role of molecular switch for triggering shape memory effect. The network chains are flexible and therefore the polymers can develop large deformation at temperature above T_{trans}. In contrast, they are frozen to lose mobility and the polymers thus can be fixed in a temporary shape at temperature below T_{trans}. The network chains of SMPs can be crystalline (T_{trans} is a melting temperature T_m) or amorphous (T_{trans} is a transition temperature T_g). SMPs can be either chemically cross-linked or physically cross-linked polymer networks. The cross-links stabilize the networks in the course of shape memorization resulting in the polymers always memorizing their original shapes. In the polymer networks of SMPs, the chemical cross-links are covalent bonds while the physical cross-links can be phase aggregations or molecular entanglements [15]. The network

* Corresponding author.
E-mail address: tchujl@polyu.edu.hk (J.L. Hu).

0032-3861/$ - see front matter © 2007 Elsevier Ltd. All rights reserved.
doi:10.1016/j.polymer.2007.06.032

chains and cross-links of the physically cross-linked SMPs were often comprised of different phases. The phases serving as network chains and cross-links were conventionally called ''reversible phase'' and ''fixed phase'', respectively.

Due to their promising applications and flexible molecular design, shape memory polyurethanes (SMPUs) have drawn the most attention in the SMPs since certain segmented polyurethanes were found to show shape memory effect [2,4,19]. As well known, the hard- and soft-segment in segmented polyurethanes tend to separate into hard-segment and soft-segment phases due to their thermodynamical dissimilarity. In general, the hard-segment and the soft-segment phases in the segmented polyurethanes with shape memory effect play the roles of fixed phase and reversible phase, respectively [2,7]. The morphology of the phase separation, phase composition, microdomain sizes, phase distribution, and so on underlies the structure of physically cross-linked networks and shape memory properties of the SMPUs. The relationship between morphology and shape memory properties is essential for optimizing the molecular design and applications of SMPUs.

A few attempts have been made to investigate the segmented polyurethanes with shape memory effect. Hayashi and coworkers from Mitsubishi Heavy Industry Ltd (MHI) developed SMPUs with amorphous reversible phase [19,20]. However, they did not elucidate the relationship between structure and shape memory effect of the polyurethanes. Lin had prepared a series of segmented polyurethanes with amorphous reversible phase [4,5]. Kim [7] synthesized a series of shape memory polyurethanes having crystalline reversible phase. They investigated the influences of soft-segment length and hard-segment content on shape memory effect. But the polyurethanes in their studies were either in a narrow range of composition or in a wide range of composition in which the two successive composition levels were rather larger for correlating morphological structure to shape memory effect. Therefore the relationship between morphological structures and shape memory properties is still open for investigations. In addition, the thermomechanical conditions in terms of deformation amplitude, temperature, time, speed could greatly influence the shape memory behaviors [21]. The segmented polyurethanes with different structure would show different property dependency on the thermomechanical conditions. This has not been reported yet.

The morphology of segmented polyurethanes has been extensively investigated [22–26]. However, the morphology of the segmented polyurethanes having crystalline soft-segment phase has not been studied in details [26–29]. In particular, the microdomain morphology of the hard-segment domains in the segmented polyurethanes having crystalline soft-segment phase has not been reported. The effect of morphology of the segmented polyurethanes on their mechanical properties including modulus, strength, hysteresis and so on has also been investigated widely [30–33]. But the shape memory effect in terms of shape recovery and shape fixity is apparently different from the properties mentioned above. The relationship between the morphology and shape memory properties has remained unknown.

In view of the open area, a series of studies on the relationship between the morphology and the shape memory behaviors of the segmented polyurethanes were carried out. The author synthesized a set of segmented polyurethanes with a wide composition range in which the polyurethanes were expected to have interconnected, isolated and no hard domains. The crystalline polycaprolactone diols (PCL) were employed as the soft-segments of the polyurethanes. The crystalline soft-segment phase would play the role of reversible phase and thus it's melting transition temperature serves as the transition temperature for triggering shape memory effect, i.e., $T_{trans} = T_m$. The investigations of SMPUs with $T_{trans} = T_g$ will be presented elsewhere. The morphology of the SMPUs were studied with differential scanning calorimetry (DSC), small angle X-ray scattering (SAXS), thermomechanical analysis (TMA) and tensile hysteresis tests. The morphological changes, especially the changes of the hard-segment domains, with the chemical compositions were therefore experimentally determined. The shape memory behaviors were investigated through a series of thermomechanical cyclic tensile tests. The shape memory effect was discussed with regard to their relationship of the morphological structure. The authors believe that this series of studies will fill in the gap of understanding the shape memory effect of segmented polyurethanes and they will also benefit the study of other physically cross-linked SMPs.

2. Experimental

2.1. Materials

The polyurethanes were synthesized with PCL (Daicel) of molecular weight 4000 (hereafter called PCL4000) as the soft-segments, 4,4′-diphenylmethane diisocyanate (MDI, Acros) as the chain extender and 1,4-butanediol (BD, International Laboratory) as the hard-segments. The PCL4000 was dried and dehydrated at 80 °C under vacuum for 6 h prior to be used. The solvent *N*,*N*′-dimethylformamide (DMF) from Aldrich was dried with 4 Å molecular sieves. A two-step polymerization was employed. The isocynate-terminated prepolymers were first prepared by reacting the dried PCL4000 with the mole excessive MDI to ensure complete reaction in the DMF solution at 65 °C for 3 h. Then the prepolymers were chain extended with BD at 80 °C for another 4 h. The molecular characteristics of the polyurethane samples are shown in Table 1. The series of samples are designated as PU-XX where XX stands for the hard-segment content (HSC). The polyurethane films were fabricated by casting the polyurethane solutions into a rectangular Teflon mold and drying in a vacuum oven at 80 °C for 24 h. To eliminate the thermal history, the films were heated up to 120 °C in a furnace and was cooled to room temperature slowly in another 24 h. The thickness of the films was about 0.2 mm–0.4 mm.

2.2. Characterizations

The thermal properties of the polyurethanes were investigated with DSC (Perkin-Elmer, Diamond). During the

Table 1
Polyurethane samples characteristics

Samples	HSC (wt%) (MDI + BDO)	Density at 65 °C (g/cm^3)	Theoretical volume fraction of hard-segment	Average number of MDI per hard-segment	Average number of BD per hard-segment
PU-10	10	1.090	0.076	1.41	0.41
PU-15	15	1.106	0.124	2.22	1.22
PU-20	20	1.120	0.167	2.97	1.97
PU-25	25	1.133	0.211	3.91	2.91
PU-30	30	1.143	0.256	4.98	3.98
PU-35	35	1.155	0.302	6.32	5.32
PU-40	40	1.170	0.349	7.66	6.66
PU-45	45	1.182	0.397	9.36	8.36
PU-50	50	1.199	0.446	11.40	10.40

experiment, it was purged with nitrogen gas and cooled with an intracooler. The samples scanned from −50 °C to 250 °C at a scanning rate of 10 °C or 50 °C/min.

The thermomechanical analysis was conducted with the Perkin-Elmer TMA7. The tests were performed at a scanning rate of 10 °C/min from 0 °C to 220 °C in penetration mode with a probe load of 50 mg.

The tensile hysteresis properties of the polyurethane films were tested at $T_m + 20$ °C on a universal material tester Instron 4466 which was equipped with a temperature-controlled chamber. Here T_m represented the melting transition temperature of soft-segment phase of the polyurethanes. The samples for the tensile hysteresis tests were 60 mm long and 5 mm wide. A series of cyclic tensile tests with the strain increasing from 50% to 400% were conducted. The samples were loaded and unloaded at a constant speed of 50% strain/min. The percentage of hysteresis for a given cycle was calculated by the ratio of the area bounded by the loading-unloading curves to the total area under the loading curve.

SAXS experiments were performed on a special equipment Nanostar (Bruker) which was equipped with a heating accessory produced by Anton Paar Co. This equipment employs Cu Kα ($\lambda = 0.154$ nm) as the radiation source. The collimation system consisted of two cross coupled Gobel Mirrors and four pinholes. The detector was a Bruker AXS HI-STAR position sensitive area detector. The diameter of the incident beam was about 1 mm. The sample to detector distance was 1.061 m. The polyurethanes were heated up to $T_m + 20$ °C. In order to ensure the complete melting of crystalline soft-segment phase, the polyurethanes were kept at $T_m + 20$ °C for 10 min. Subsequently, the SAXS tests of the polyurethanes were performed at $T_m + 20$ °C. The time for each test was 1 h and the scattering range was $q = 0.1\ \text{nm}^{-1}$–$2.0\ \text{nm}^{-1}$ where $q = (4\pi/\lambda)\sin(\theta/2)$ was the scattering vector of the scattering angle θ. The relative scattering intensity $I(q)$ was converted to absolute intensity by the absolute calibration with pure water as the secondary standard [34]. The data were then corrected for background noise and thermal density fluctuations. The background caused by thermal density fluctuation was estimated via a q independent method and the background intensity I_B was taken as a constant [35]. The mass density of the polyurethane films was measured in nonane at $T_m + 20$ °C in a floatation way.

Wide angle X-ray diffraction (WAXD) profiles of the polyurethanes were collected with Philips Xpert XRD System (Cu Kα) operated at 40 kV and 20 mA. The measurements were performed in the range of 2θ from 10° to 35° at a rate of 0.03 sec/step.

The shape memory effect of the polyurethanes was measured through three sets of thermomechanical cyclic tensile tests which were conducted on the Instron 4466 [21]. The properties of a polyurethane film were obtained from the averaging of the results of five specimens tested under the same conditions. In the first set of tests, samples of the polyurethane film were loaded and elongated to 100% strain at a speed of 50%/min under the temperature $T_m + 20$ °C at first. Subsequently the samples were quenched to the temperature $T_m - 20$ °C and unloaded. In the unloading process the stress started to be zero at a certain strain that was taken as the fixed strain and shape fixity thus could be calculated. Then the samples underwent the recovery process by being heated at the recovery temperature $T_m + 20$ °C for 15 min. Afterwards, the next cycle started. In the second loading process, the stress started to be more than zero at a strain that was considered as the residual strain in the preceding cycle. The shape recovery in the preceding cycle can thus be calculated. The second set of tests was merely different from the first set tests with this step: at the end of the extension, the polyurethanes were maintained at $T_m + 20$ °C for 30 min before being cooled down to $T_m - 20$ °C. In the third set of tests, the deformation temperature and recovery temperature were $T_m + 10$ °C while the shape fixing temperature was still located at $T_m - 20$ °C. The deformation amplitude increased from 50% to 250% with an interval of 50%. The shape fixity (R_f) and the shape recovery (R_r) are calculated with the following equations:

$$R_f = \frac{\varepsilon_u}{\varepsilon_m} \times 100\% \quad (1)$$

$$R_r = \frac{\varepsilon_m - \varepsilon_p}{\varepsilon_m} \times 100\% \quad (2)$$

where ε_m denotes the maximum strain in the cyclic tensile tests; ε_u is the residual strain after unloading at $T_m - 20$ °C and ε_p is the residual strain after shape recovery.

The effect of the recovery temperature on the shape recovery of the specimens was investigated on a Nikon Microscope

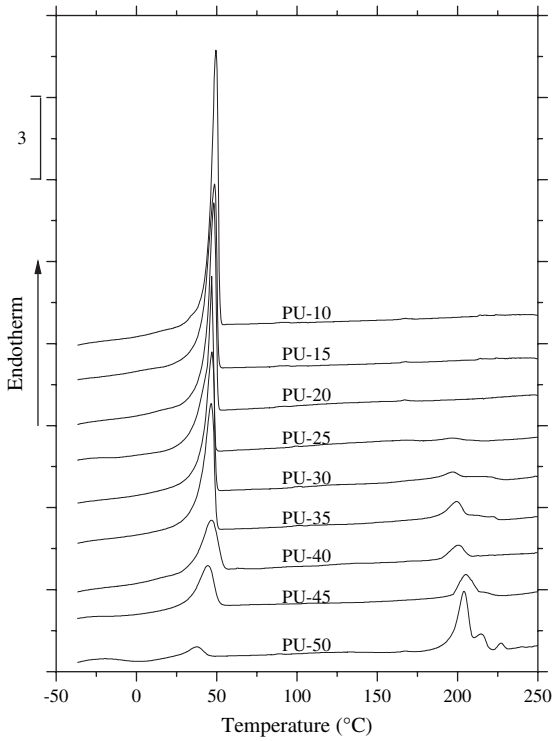

Fig. 1. DSC thermograms of polyurethanes at a scanning rate of 10 °C/min.

equipped with a hot stage. At first, the polyurethane specimens were extended to a strain followed by cooling down to frozen state. Then the deformed specimens were fixed on the hot stage of the microscope. By heating the specimens at a rate of 2 °C/min the course of shape recovery was observed and recorded under the microscope. At a temperature T_∞ the shape recovery started to stop increasing and the tests were accomplished. The shape recoveries of the specimens were calculated through Eq. (2).

3. Results

3.1. DSC

As mentioned above, the DSC samples were the polyurethane films prepared after the annealing from 120 °C to room temperature in 24 h. Hence it was assumed that the thermal history of the specimens has been mostly eliminated. Fig. 1 presents the DSC traces of the segmented polyurethanes. All the samples showed endothermic peaks in the range of 40 °C–50 °C which revealed the melting of the crystallites of soft-segments PCL4000. The polyurethanes with higher HSC exhibited endothermic peaks in the vicinity of 200 °C which were attributed to the melting of the hard-segment phase. This manifested the existence of hard-segment phase in these samples. With the increase of HSC, the endothermic peaks pertaining to the hard-segment phase were intensified while those representing the soft-segment phase were weakened. It indicated that increasing HSC resulted in the decrease of the crystallinity of the soft-segment phase. Table 2 shows the melting temperature and the heat of fusion of the polyurethanes. Under the same conditions, the DSC test was performed on the pure PCL4000. The melting temperature and the heat of fusion of pure PLC4000 were found to be 52.3 °C and 84.12 J/g, respectively. The melting temperatures of the soft-segment phase of the polyurethanes were slightly lower than that of the pure PCL4000. The crystallinity of soft-segments of the samples could be calculated from the ratio of the heat of fusion of the soft-segment phase to that of the pure PCL4000. As shown in Table 2, the crystallinity of soft-segment phase decreased with the increase of HSC and dramatically reduced when HSC $\geq$ 40%. The melting temperature and the heat of fusion of hard-segment phase increased with the increase of HSC.

In the foregoing DSC test results, PU-15 and PU-20 showed almost no endothermic peaks of the hard-segment phase, but the sample PU-25 seemed to show a weak endothermic behavior. To verify these observations, DSC tests at a higher scanning rate of 50 °C/min were performed on the polyurethanes PU-20, PU-25 and PU-30. The results are given in Fig. 2. It was found that PU-25 and PU-30 exhibited endothermic peaks of the hard-segment phase but PU-20 did not. It suggested that the polyurethanes having over 25% of HSC possessed hard-segment domains whereas PU-20 had no hard-segment domains. However, from the TMA and SAXS tests, PU-15 and PU-20 were manifested to still contain more or less hard-segment phase that might be out of the sensitivity of the DSC technique.

Table 2
DSC testing results (10 °C/min)

Samples	T_m (°C)		Heat of fusion δH_m (J/g)		Crystallinity of soft-segments (%)
	Soft-segments	Hard-segments	Soft-segments	Hard-segments	
PU-10	49.53	–	47.14	–	56.04
PU-15	48.70	–	45.56	–	54.16
PU-20	48.03	–	44.74	–	53.18
PU-25	46.87	195.87	35.51	1.15	42.21
PU-30	46.53	196.70	32.82	1.71	39.01
PU-35	44.70	199.37	31.19	2.16	37.07
PU-40	42.53	199.87	18.71	4.45	22.24
PU-45	42.20	200.43	15.07	4.66	17.91
PU-50	37.40	203.87/215.34/226.87	3.82	8.03/0.92/0.54	4.54

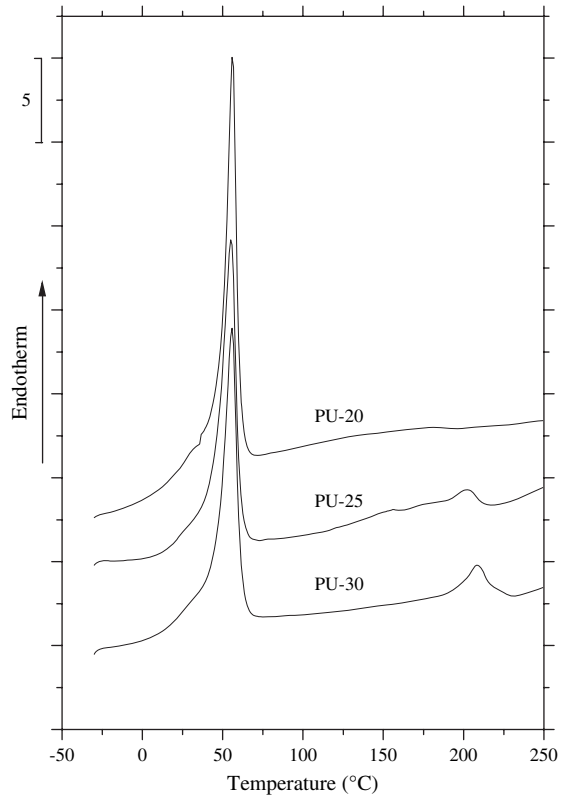

Fig. 2. DSC thermograms of the samples PU-20, PU-25 and PU-30 at a scanning rate of 50 °C/min.

4. TMA

The TMA traces for the segmented polyurethanes are shown in Fig. 3. The polyurethanes exhibited two softening transitions. The transition located in the temperature range 40 °C–50 °C corresponded to the softening of the soft-segment phase. This was consistent with the DSC results. The transition that took place in the higher temperature range 90 °C–200 °C was attributed to the softening of hard-segment phase. All the segmented polyurethanes except PU-10 showed more or less a platform before the softening of the hard-segment phase. PU-10 did not exhibit platform and the softening transition of hard-segment phase. This seemed to suggest that PU-10 formed no hard-segment domains whereas the other polyurethanes possessed hard-segment domains. It was also found that the softening transition of the hard-segment phase shifted to high temperature as the HSC increased. This could be ascribed to the increasing order and purity of the hard-segment phase with the increase of HSC. PU-45 and PU-50 showed no softening transition of the soft-segment phase. It suggested that the hard-segment phase changed from an isolated state to an interconnected state; or from a discontinuous phase to a continuous phase in such a HSC range. The interconnected hard-segment phase formed a rigid framework which prevented the polymer from softening when the soft-segment phase melted.

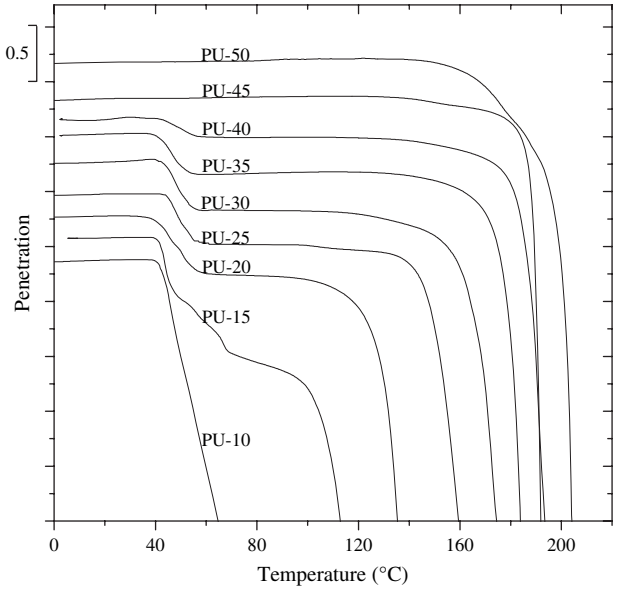

Fig. 3. TMA thermograms of the polyurethane at a scanning rate of 10 °C/min.

4.1. Tensile hysteresis

In order to manifest this morphological change of the hard-segment phase, the tensile hysteresis tests were conducted on the polyurethane samples at the temperature of $T_m + 20$ °C to ensure all the crystallites of soft-segments melted completely. As shown in Fig. 4, the values of percent hysteresis of PU-30, PU-35 and PU-40 were about 40% while those of PU-45 and PU-50 were substantially increased. This was attributed to the interconnecting of the hard-segment domains in PU-45 and PU-50. In response to the applied tensile stress, the interconnected hard-segment phase in these polymers would deform at the beginning of deformation, which lead to an increase of plastic deformation and consequently gave rise to higher percentage of hysteresis.

5. SAXS

A great number of researchers have employed SAXS to investigate the morphology of polyurethanes with amorphous soft-segment phase [22–24,35,36]. But few investigations

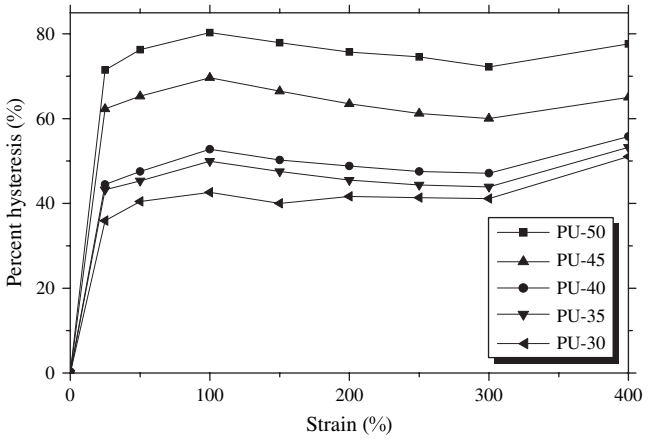

Fig. 4. Percent hysteresis of the polyurethanes under tensile tests at $T_m + 20$ °C.

have been made on the morphology of the polyurethanes with crystalline soft-segment phase. Cooper studied the morphology of polyurethanes having crystalline PCL as soft-segments with SAXS at room temperature [22]. The author considered that the polyurethanes could be treated as ''pseudo two-phase system'' due to the apparent difference between the soft and hard-segments. The polyurethanes were therefore mathematically analyzed based on the two-phase models. However, for segmented polyurethanes with high crystallinity of soft-segment phase, the two-phase models would not be appropriate because at room temperature the polyurethanes would contain a great number of crystallites of soft-segments whose contribution to the x-rays scattering could not be neglected any more. In this study, the scattering tests of the polyurethanes were performed at $T_m + 20$ °C in order to ensure the complete melting of the crystallites of the soft-segment phase. The polyurethanes mainly possessed hard-segment and amorphous soft-segment phases at $T_m + 20$ °C. Thereby the polyurethanes could be approximately viewed as ''two-phase system''.

The SAXS profiles of the polyurethanes are presented in Fig. 5. The polyurethanes showed scattering peaks or shoulders except PU-10. This implied that PU-10 was basically homogeneous while the other polyurethanes exhibited more or less phase separation. It could be concluded that all the polyurethane samples possessed the hard-segment domains except PU-10. This was in agreement with the results obtained in the TMA tests. In the polymerization one MDI group could react with two PTMO diols, creating what we will subsequently refer to as ''lone'' MDI unit. The average number of BD per hard-segment of PU-10 is only 0.4 as shown in Table 1. Hence there should be a higher percentage of lone MDI groups in PU-10 as compared with the other polyurethanes. These lone MDIs introduce no urethane groups and are at least 100 bonds away from another MDI unit in the chain. Consequently, these species would not be expected to be associated with the hard domains but located in the soft-segment phase. Hence the polyurethanes PU-10 unlikely formed hard-segment domains.

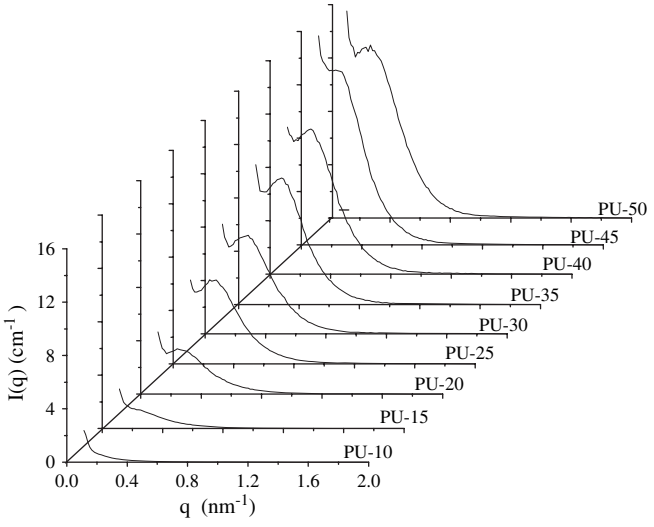

Fig. 5. SAXS profiles of the polyurethanes at $T_m + 20$ °C.

Table 3
Interdomain spacings and domain sizes of the segmented polyurethanes

	Interdomain spacings (nm)	Domain sizes	
		$\bar{l}_H$ (nm)	$\bar{l}_S$ (nm)
PU-10	–	–	–
PU-15	25.1	2.6	18.9
PU-20	24.1	2.6	13.4
PU-25	23.4	2.8	10.8
PU-30	23.5	2.9	8.7
PU-35	23.0	3.4	8.1
PU-40	22.8	3.6	6.9
PU-45	23.8	3.5	5.5
PU-50	22.8	3.6	4.9

According to the Bragg's law, the three dimensional interdomain spacing can be obtained from the maximum of the scattering profiles. Table 3 summarizes the interdomain spacings of polyurethanes obtained by both Bragg's law. The results revealed that for the polyurethanes with HSC ranging from 10% to 40%, the interdomain spacing generally decreased with the increase of HSC. With further increase of HSC, the interdomain spacing of PU-45 increased obviously followed by a decrease of the PU-50. This could be ascribed to the transition of hard domains changing from isolated to interconnected state. The decrease of the interdomain spacing with the increase of HSC meant the increase of the number of hard-segment domains and the increase of the cross-linking density of the physical networks.

In addition to the interdomain spacing, the domain sizes of the samples have been estimated from the SAXS results. This was accomplished by applying the Porod's law to the SAXS profiles. The Porod's law is described by Eq. (3),

$$\lim_{q\to\infty} I(q) = \frac{K}{q^4} \tag{3}$$

where K is the Porod constant. Taking into account the influence of the background I_B caused by the phase mixing within phases the observed scattering intensity $I_{obs}(q)$ is given by:

$$\lim_{q\to\infty} I_{obs}(q) = \lim_{q\to\infty} \frac{K}{q^4} + I_B \tag{4}$$

The background corrected intensity is therefore equal to considering $I_{obs}(q) - I_B$. By considering the effect of diffuse boundary between the hard-segment and soft-segment domains, the background corrected intensity is modified as:

$$\lim_{q\to\infty} I(q) = \lim_{q\to\infty} \frac{K}{q^4} \exp\left(-\sigma^2 q^2\right) \tag{5}$$

where σ is a measure of the interfacial boundary thickness. The Porod constant K is related to the interfacial surface-to-volume ratio (S/V) through the equation:

$$\frac{S}{V} = \pi\phi_H\phi_S\frac{K}{\int_0^\infty I(q)q^2\mathrm{d}q} \quad (6)$$

where ϕ_H and ϕ_S denote the theoretical volume fraction of the hard-segment and soft-segment phases, respectively. The average length of hard-segment $\bar{l}_H$ and soft-segment domains $\bar{l}_S$can be calculated from the equation:

$$\bar{l}_H = 4\phi_H/\left(\frac{S}{V}\right);\ \bar{l}_S = 4\phi_S/\left(\frac{S}{V}\right) \quad (7)$$

The domain size obtained from Porod' law and the correlation function $\gamma_1(r)$ are presented in Table 3. It was found that the size of hard-segment domains generally increased with the increasing HSC. On the contrary, the sizes of soft-segment domains increased with the decrease of HSC. The increasing tendency was particularly apparent in the range of low HSC. This suggested that the cross-linking density of the polyurethanes with low hard-segment content was much lower than that of the ones with high HSC.

5.1. Shape memory effect

At first, the shape memory effect was measured from the first set of thermomechanical cyclic tensile tests mentioned above. Fig. 6 shows the shape memory effect of the segmented polyurethanes changing with HSC. It can be seen that the shape fixity decreased with the increase of HSC. When HSC $\leq$ 35% the polyurethanes showed over 94% of shape fixity while when HSC $\geq$ 40% the shape fixity decreased rapidly. The previous investigations considered that the crystallization of soft-segments determined the shape fixing of the shape memory polyurethanes [2,7]. In order to understand effect of the crystallization on shape fixity, three sets of WAXD tests were performed on the polyurethane films before extension, after shape fixing and after shape recovery to trace the crystallinity changes that happened to these segmented polyurethanes in the course of shape memorization.

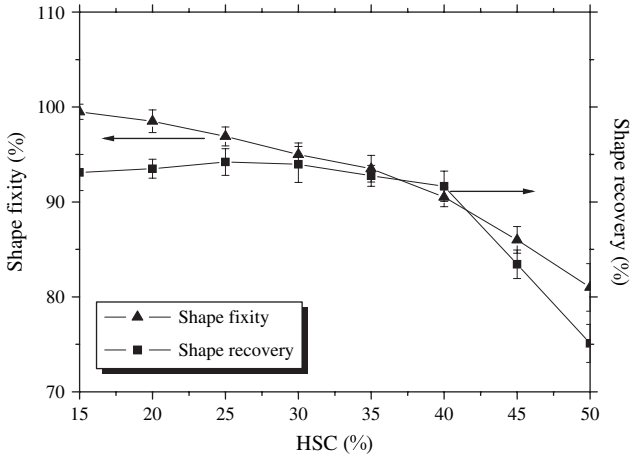

Fig. 6. Shape memory effect as a function of HSC.

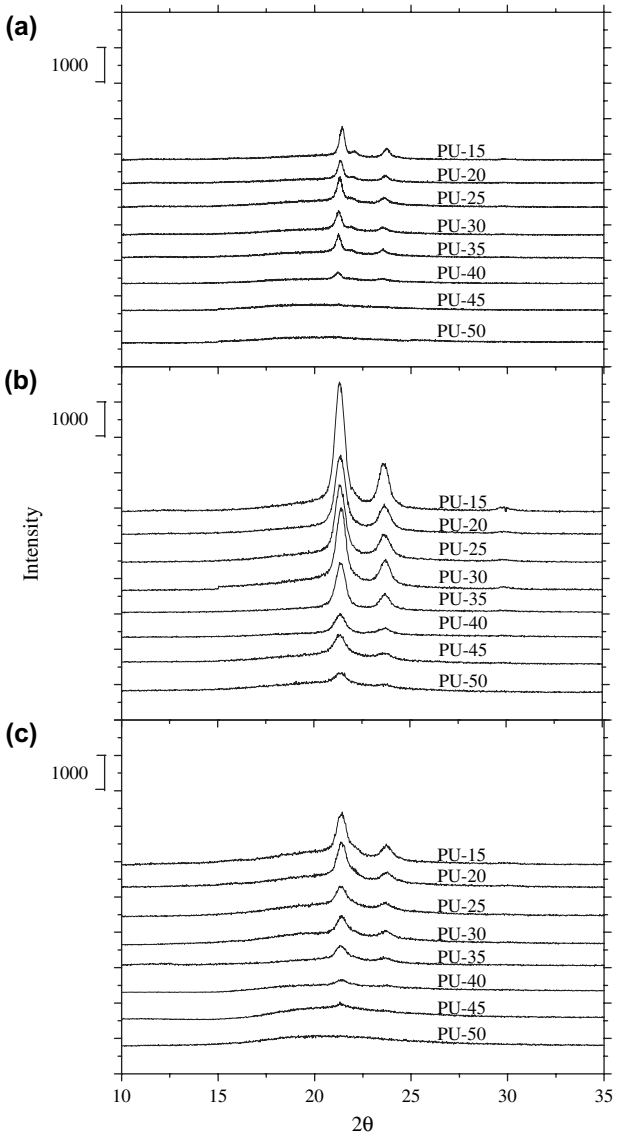

Fig. 7. Tracing the structural changes taken place to the polyurethanes in a cycle of shape memorization by the WAXD tests at room temperature: (a) before extension; (b) after shape fixing (being extended 100% and fixed in a temporary shape); (c) after shape recovery.

As shown in Fig. 7a, before extension the polyurethanes with HSC $\leq$ 40% showed the diffraction peaks which were ascribed to the crystallization of the soft-segment phase [7]. The intensity of the diffraction peaks decreased with the HSC increase. This suggested that the crystallinity of soft-segment phase of the polyurethanes decreased gradually as HSC increased. When HSC increased to 45% and 50% the diffraction peaks disappeared, which proved that the soft-segments were amorphous in PU-45 and PU-50. As shown in Fig. 7b, the intensity of the diffraction peaks of the polyurethanes increased substantially after shape fixing and even PU-45 and PU-50 showed weak diffraction peaks. Because the position of the diffraction peaks was identical to those shown in the WAXD tests before extension the peaks were still ascribed to the crystallization of soft-segment phase. The increase of the crystallinity was attributed to the strain-induced crystallization that

took place to soft-segments after extension and shape fixing. The crystallinity of the polyurethanes still decreased with the increase of HSC. The crystallinity of PU-40, PU-45 and PU-50 was much lower than that of the other polyurethanes. This was why the shape fixity dropped rapidly when HSC $\geq$ 40%. In contrast, the high shape fixity of the polyurethanes with HSC $\leq$ 35% would result from their high crystallinity after shape fixing. As shown in Fig. 7c, the polyurethanes after shape recovery showed a little higher diffraction intensity as compared with the polyurethanes before deformation. This implied that after a cycle of shape memorization the soft-segments oriented partially resulting in a slight increase of crystallinity even though the polyurethanes almost recovered to their original shape.

As mentioned above, the shape recovery of the segmented polyurethanes was determined by the physically cross-linked network maintained in the course of shape memorization. Fig. 6 shows the shape recovery as a function of HSC. The segmented polyurethanes with 15% $\leq$ HSC $\leq$ 40% showed over 90% of shape recovery. However, as HSC increased to 45% and 50% the shape recovery dramatically dropped to 83% and 75%. This decrease of shape recovery should result from the hard-segment phase changing from isolated to interconnected states. Since the interconnected hard-segment domains in PU-45 and PU-50 formed rigid framework the hard-segment phase should be enforced to take place large deformation in the extension. This resulted in the lower shape recovery of the two polyurethanes at this recovery temperature.

In the evaluation of shape memory effect, the thermomechanical cyclic tensile tests were extensively employed. The method could indeed provide highly reproducible experimental results [2]. As described previously, the shape fixity was obtained in the unloading process and the shape recovery was extracted from the loading processes after the first cycle. However, the author found that if the segmented polyurethanes were continuously kept at $T_m - 20$ °C after unloading their shape fixity would decrease gradually. The similar phenomena was also observed in an investigation about a shape memory polyurethane with $T_{trans} = T_g$ [37]. In the present study, the shape fixity of these polyurethanes changing with the time was shown in Fig. 8. The shape fixity decreased greatly at the time of 15 min after unloading. Furthermore the decreasing tendency rose with the HSC increase. The shape fixity tended to stabilize at certain values when the samples were maintained at $T_m - 20$ °C for 90 min and 120 min after unloading.

In the previous thermomechanical cyclic tensile tests the shape recovery of the polyurethanes took place at $T_m + 20$ °C. To examine the influences of recovery temperature on the shape recovery, a series of shape recovery tests were performed on a Nikon Microscope equipped with a hot stage. Fig. 9 presents the shape recovery of the polyurethanes with varying HSC as a function of recovery temperature. The starting shape recovery of the segmented polyurethanes corresponds to the shape fixity obtained when they were kept at $T_m - 20$ °C for 120 min after unloading. For example, PU-50 remained with 65% shape fixity in this case and it's starting shape recovery in Fig. 9 is 35%. It was found that the all the segmented polyurethanes showed over 90% of shape recovery when they were heated up to T_∞. All the segmented polyurethanes showed abrupt increase of shape recovery in a narrow temperature range around T_{trans}. The shape recovery in this stage resulted from the melting transition and recovery of the soft-segment phase. After the stage the rate of shape recovery apparently slowed down and the segmented polyurethanes with HSC $\leq$ 40% almost recovered to their original shape. In contrast, PU-45 and PU-50 showed apparent shape recovery after the melting transition of soft-segment phase. The shape recovery after melting transition was mainly ascribed to the recovery of the deformed hard-segment phase. At the recovery temperature of $T_m + 20$ °C, the shape recovery of PU-45 and PU-50 was much lower than that of the other segmented polyurethanes. This was consistent with the experimental results of the previous thermomechanical cyclic tensile tests. The lower shape recovery of the PU-45 and PU-50 at $T_m + 20$ °C was mainly caused by the deformation of hard-segment phase that occurred in the extension of the segmented polyurethanes.

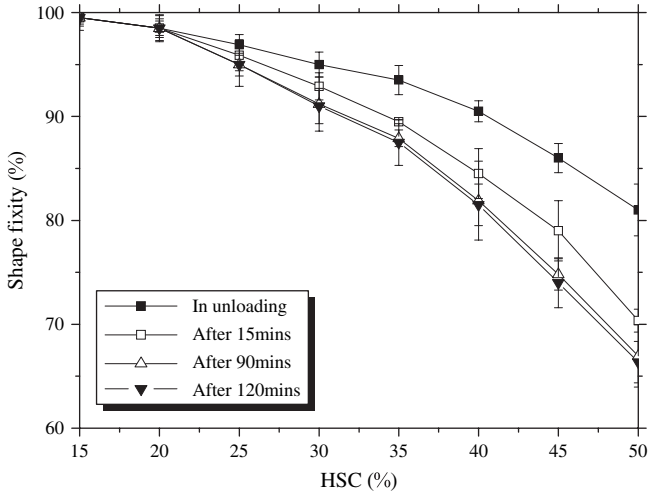

Fig. 8. Shape fixity as a function of time at $T_m - 20$ °C.

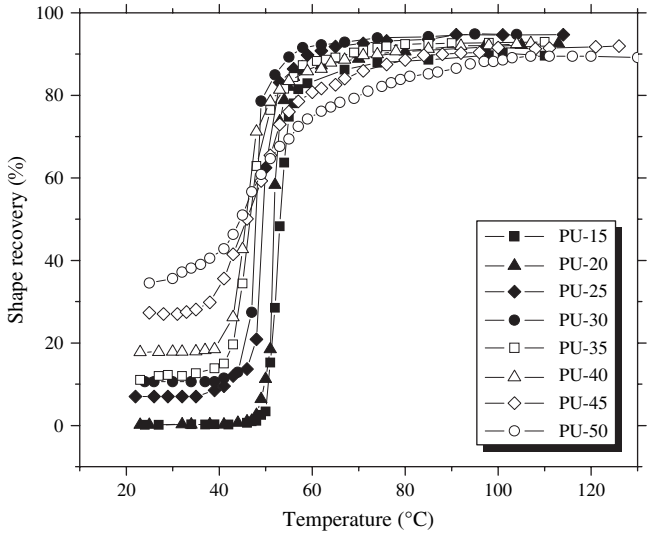

Fig. 9. Shape recovery as a function of recovery temperature.

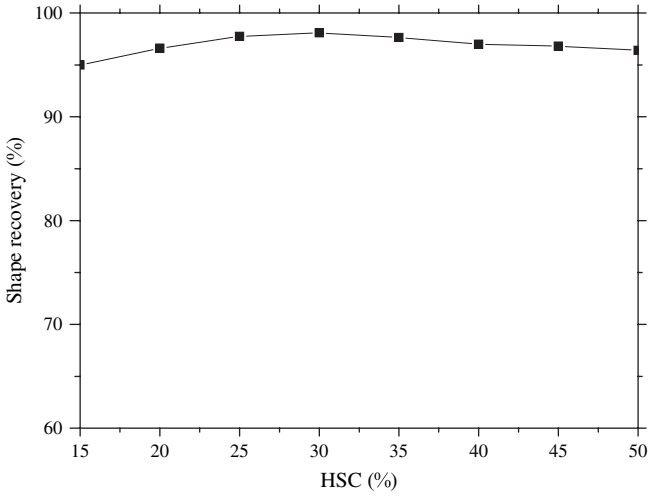

Fig. 10. Final shape recovery of the segmented polyurethanes.

To eliminate the effect of the thermal expansion, the recovered segmented polyurethanes were cooled down to room temperature and the final strains were measured. As shown in Fig. 10, the final irreversible deformation of all the segmented polyurethanes was less than 5% and the ultimate shape recovery of the segmented polyurethanes was over 95%. The tests indicated that the deformation of hard-segment phase could mostly be recovered if the segmented polyurethanes were heated to sufficiently high temperature. Therefore deformation of hard-segment phase was basically viscoelastic other than plastic deformation. From the shape recovery tests it was inferred that the shape fixity of the segmented polyurethanes with lower HSC was mainly ascribed to the strain-induced crystallization of soft-segment phase while that of the segmented polyurethanes with higher HSC, particularly PU-45 and PU-50 consisted of both the strain-induced crystallization of soft-segment phase and the deformation of hard-segment phase.

The deformation of the polymers consists of elastic deformation, viscoelastic deformation and irreversible deformation [38]. The total deformation ε of the segmented polyurethanes with higher HSC can be given by Eq. (8)

$$\varepsilon = \varepsilon_e + \varepsilon_{vis} + \varepsilon_{ir} \approx \varepsilon_{vis} + \varepsilon_{ir} \tag{8}$$

where ε_e, ε_{vis} and ε_{ir} stand for elastic deformation, viscoelastic deformation and irreversible deformation, respectively. Since the ε_e is usually negligibly small the total deformation ε is approximately composed of ε_{vis} and ε_{ir}. The foregoing shape recovery tests proved that ε_{ir} was less than 5%. Hence the deformation of the segmented polyurethanes in this study was determined by the viscoelastic deformation ε_{vis} which included the viscoelastic deformation of soft-segment phase ε_{vis}(SS) and hard-segment phase. ε_{vis}(HS). The shape fixing and shape recovery were just tightly related to the ε_{vis}(SS) and ε_{vis}(HS). The distribution of viscoelastic deformation between soft-segment and hard-segment phases was dependent on the two-phase morphology including phase separation, phase volume fraction, domain nature, size, number and connectivity, and so on. Thus the shape memory effect was defined by the two-phase morphological structure.

5.2. Influences of stress relaxation

It is impossible to avoid stress relaxation entirely in the course of shape memorization of thermoplastic SMPs. For example, the SMPs may not always be quickly cooled down to frozen state in practical applications due to the limitation of cooling and heat transfer efficiency. In some cases, they may be maintained in the constraint state at a high temperature above T_{trans} for a long time and the stress relaxation can thus undergo greatly. It was found that the stress relaxation would bring to the decrease of shape recovery of a SMPU in one of our previous study [23]. It is assumed that the polyurethanes with different structures will show different dependency on the stress relaxation. In this study, the influences of stress relaxation on the shape memory effect of the polyurethanes with varying HSC were investigated. For this purpose, the second set of thermomechanical cyclic tensile tests were performed on the segmented polyurethanes. As the forgoing description the segmented polyurethanes were cooled down to $T_m - 20\,^{\circ}C$ at once after extension in the first set of tests while they were maintained in the constraint state at $T_m + 20\,^{\circ}C$ for 30 min before cooling in the second set of tests. The polyurethanes could undergo more stress relaxation in the second set of tests than they did in the first set of tests. The effect of stress relaxation on the shape fixity of the segmented polyurethanes is shown in Fig. 11. It can be seen that the stress relaxation brought increase to the shape fixity of the polyurethanes. Moreover, the increasing tendency rose with the increase of HSC.

As shown in Fig. 12, the shape recovery of all the segmented polyurethanes obtained in the second set of tests was lower than that from the first set of tests. It was also found that the decrease of shape recovery was more apparent when HSC decreased to 20% and 15%. There might be two reasons for this phenomenon. The first reason is, besides the hard-

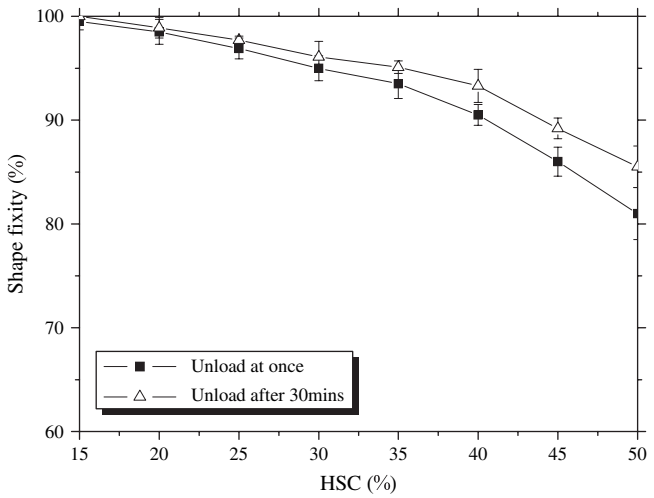

Fig. 11. Effect of stress relaxation on shape fixity.

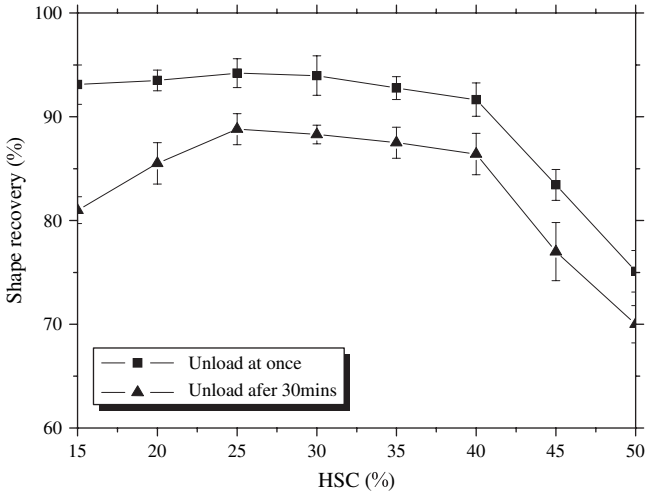

Fig. 12. Effect of stress relaxation on shape recovery.

segment domains the molecular interactions such as the intermolecular hydrogen bonds, dipole to dipole interactions, induced dipole to dipole interactions and even molecular entanglements in the polyurethanes could also prevent the molecular slippage in a short time scale [13]. SAXS results showed that the domain sizes of soft-segment phase of PU-15 and PU-20 were much larger than those of the others. The soft-segments might not be well held by hard-segment domains in the two polyurethanes. But the molecular interactions in the soft-segment domains could help to prevent molecular slippage in a short time and they should play a comparatively important role in PU-15 and PU-20. But the molecular interactions had only limited lifetime and could break and reconstruct upon the external force for a long time scale. For the second reason, in PU-15 and PU-20 some of the hard-segment domains may not be stable enough and therefore could also break and reconstruct. The instability of physical cross-links resulted in PU-15 and PU-20 showing more apparently dropped shape recovery in the tests with cooling after 20 min. In contrast, the polyurethanes with higher HSC from 25% to 50% could better resist the stress relaxation and showed comparatively lower decrease of shape recovery due to the stable hard-segment domains as the physical cross-links.

The shape recovery tests were also performed on PU-15, PU-30 and PU-45 to study the influence of the stress relaxation. The segmented polyurethane samples for these tests were prepared cooling the deformed polyurethanes to $T_m - 20$ °C at once after extension and by maintaining the deformed polyurethanes at $T_m + 20$ °C and subsequently cooling them to $T_m - 20$ °C. Hereafter the samples from the two processes were simply designated as the segmented polyurethanes without relaxation and with relaxation. Of course, the stress relaxation would happen more or less even if the deformed polyurethanes were cooled to $T_m - 20$ °C at once. Fig. 13 presents the effect of stress relaxation of the shape recovery of the segmented polyurethane samples. The segmented polyurethanes with relaxation exhibited lower shape recovery at $T_m + 20$ °C in comparison with those without relaxation, which was in agreement with the results of the preceding thermomechanical cyclic tensile tests. With the

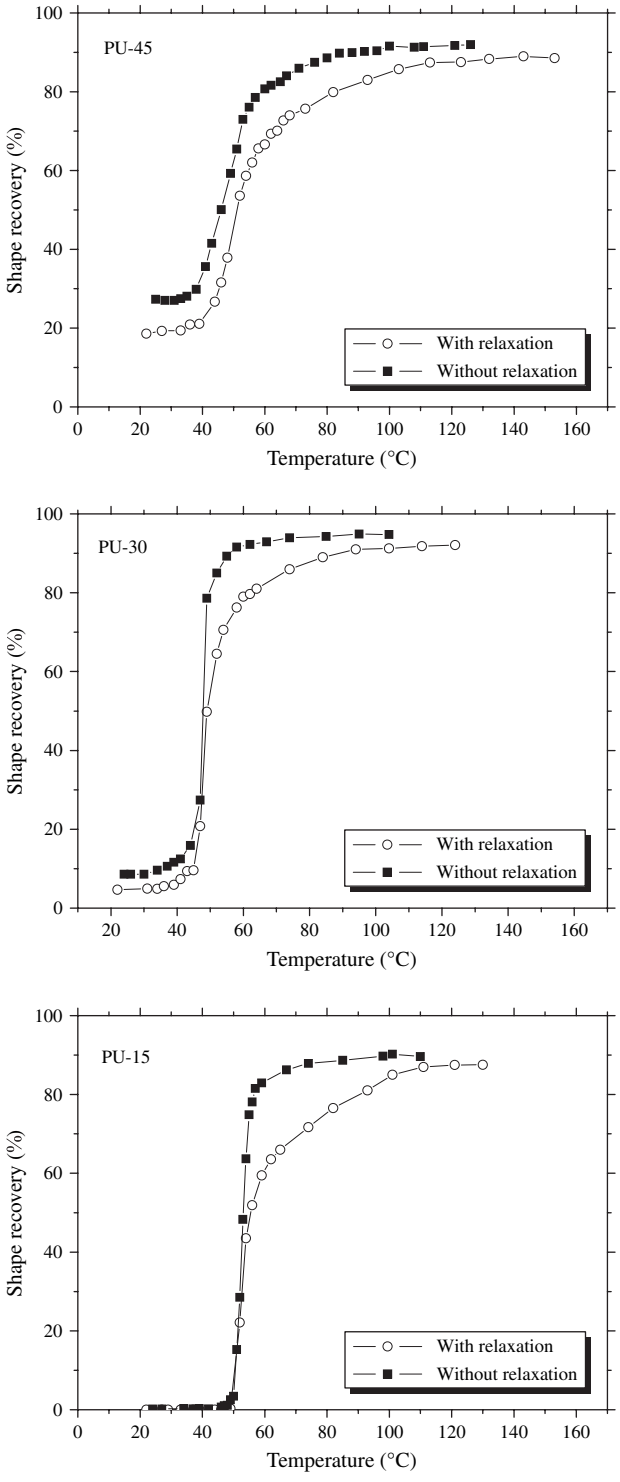

Fig. 13. Shape recovery of the samples with and without relaxation as a function of recovery temperature.

increase of recovery temperature the shape recovery of the segmented polyurethanes with relaxation would gradually increase to over 90% and the final shape recovery was close to that of the segmented polyurethanes without relaxation. Therefore it was inferred that the stress relaxation gave rise to no more irreversible deformation. It only resulted in more viscoelastic deformation of hard-segment phase or more breakage and

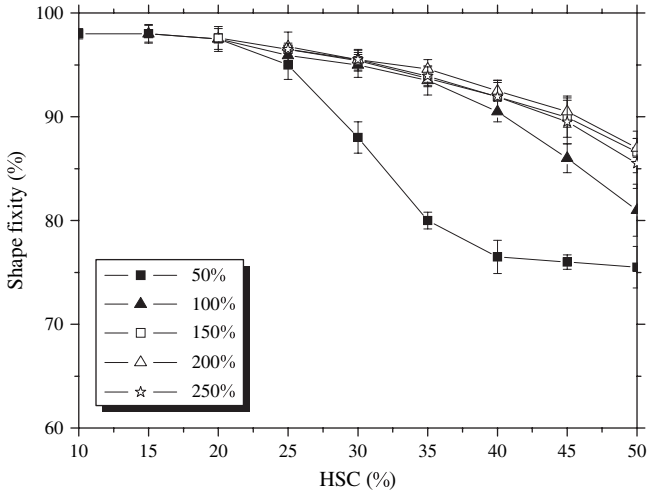

Fig. 14. Effect of deformation amplitude on shape fixity.

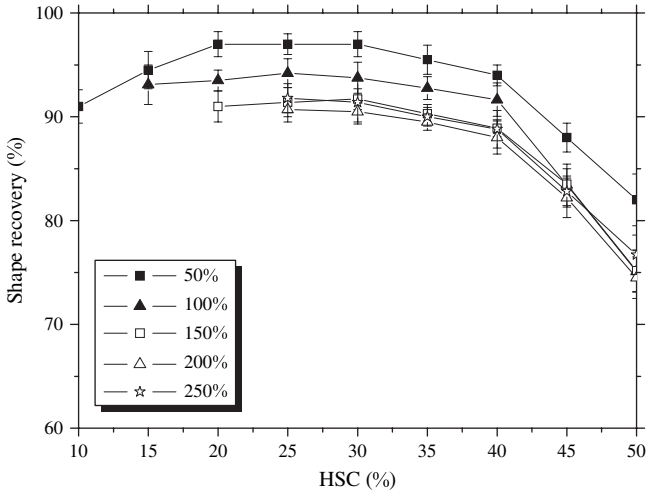

Fig. 15. Effect of deformation amplitude on shape recovery.

reconstruction of molecular interactions and instable hard-segment domains.

5.3. Influences of deformation amplitude

Fig. 14 presents the effect of deformation amplitude on shape fixity of the segmented polyurethane. It can be seen that the shape fixity rose with the increase of deformation amplitude. For all the tests with varying deformation amplitude the shape fixity decreased with the increase of HSC. This was because the crystallization capability of the soft-segments decreased with the increase of HSC. In the zone HSC $\leq$ 25%, the values of the shape fixity obtained from all the tests were over 95%. This suggested that the shape fixity of polyurethanes with low HSC was mainly determined by the high crystallinity. For the segmented polyurethanes with 30% $\leq$ HSC $\leq$ 50%, the shape fixity decreased from 95% to 76% in the tests with 50% deformation amplitude. But the values were much lower than the corresponding results obtained in the tests with 100% deformation amplitude. This seemed because the soft-segments were not fully extended with 50% deformation amplitude and no much strain-induced crystallization was developed. This implied that the polyurethanes with 30% $\leq$ HSC $\leq$ 50% had to be extended to at least over 100% strain to obtain high shape fixity. As deformation amplitude increased from 100% to 250% the shape fixity showed no apparent change when 30% $\leq$ HSC $\leq$ 35%. While in the zone 40% $\leq$ HSC $\leq$ 50% the values of the shape fixity rose gradually as deformation amplitude increased from 100% to 250%.

Fig. 15 presents the effect of deformation amplitude on shape recovery of the segmented polyurethane. For the segmented polyurethanes with 20% $\leq$ HSC $\leq$ 40%, the shape recovery decreased as the deformation amplitude increased from 50% to 200%. The decreasing tendency stopped when deformation amplitude increased to 250%. For the segmented polyurethanes with 45% $\leq$ HSC $\leq$ 50%, the shape recovery decreased as the deformation amplitude increased from 50% to 100% and did not exhibit obvious change as the deformation amplitude increased from 100% to 250%. The segmented polyurethanes having intermediate HSC of 25% and 30% showed the best shape recovery in all the tests with varying deformation amplitude. PU-35 and PU-40 showed slightly lower shape recovery. The shape recovery dropped apparently when HSC $\geq$ 45%. This resulted from larger deformation of hard-segment phase when hard-segment domains changed from isolated to interconnected state. In the tests with 50% deformation amplitude, the polyurethanes PU-20, PU-25 and PU-30 showed 97% of shape recovery. In the zone HSC $<$ 20%, the shape recovery decreased with the decrease of HSC. It was worth noting that PU-10, the polyurethane manifested to possess no hard-segment domain, still showed over 90% shape recovery. It would be the molecular interactions that prevented the molecular slippage in the deformation of PU-10 and resulted in the polyurethane memorizing it's original shape. This proved that besides hard-segment domains the molecular interaction could also play the role of physical cross-links and enable polymers to show shape memory effect under particular conditions.

The shape recovery tests were also performed on PU-25 and PU-45 to study the influence of the deformation amplitude. Fig. 16 presents the effect of the deformation amplitude on shape recovery of segmented polyurethane samples. PU-25 and PU-45 exhibited the best shape recovery at $T_m + 20\,^{\circ}C$ when the deformation amplitude was 50%, which was in agreement with the results of the foregoing tests. With the increase of recovery temperature the shape recovery of the segmented polyurethanes gradually increased to over 90%. Moreover, the segmented polyurethanes with varying deformation amplitude exhibited almost identical final shape recovery. Therefore the increase of deformation amplitude resulted in no more irreversible deformation. It indicated that the decrease of shape recovery at $T_m + 20\,^{\circ}C$ with the increase of amplitude resulted from the viscoelastic deformation of hard-segment phase or the breakage and reconstruction of molecular interactions and instable hard-segment domains.

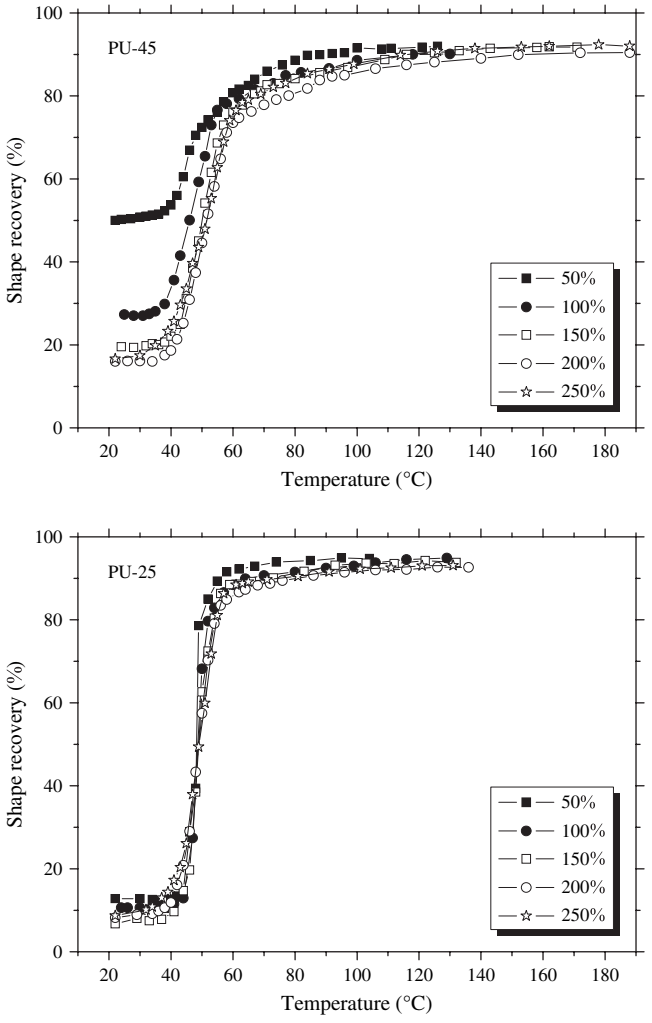

Fig. 16. Shape recovery of the samples with varying deformation amplitude as a function of recovery temperature.

5.4. Influences of pre-deformation

As a sort of smart materials, precisely controlling shape memory effect is essential for the application of SMPs. In the thermomechanical cyclic tensile tests of the segmented polyurethanes, the third loading curve was very close to second loading curve. In the other words, the segmented polyurethanes seemed turning into completely elastic after the first deformation. This fact enlightened us to enhance the shape recovery of the segmented polyurethanes by pre-deformation. In our study, the segmented polyurethanes were extended to 120% strain on the tensile tester at the $T_m + 20$ °C. Afterwards, the specimens were removed from the tensile tester and kept at the $T_m + 20$ °C for 15 min to undergo the shape recovery. Then the recovered specimen was taken as a new sample to perform the thermomechanical cyclic tensile tests with 100% deformation amplitude. As shown in Fig. 17, the shape fixity of the segmented polyurethanes was close to the case of those without pre-extension. But after the pre-deformation the shape recovery of the segmented polyurethanes was nearly 100%. It seemed because the irreversible deformation and

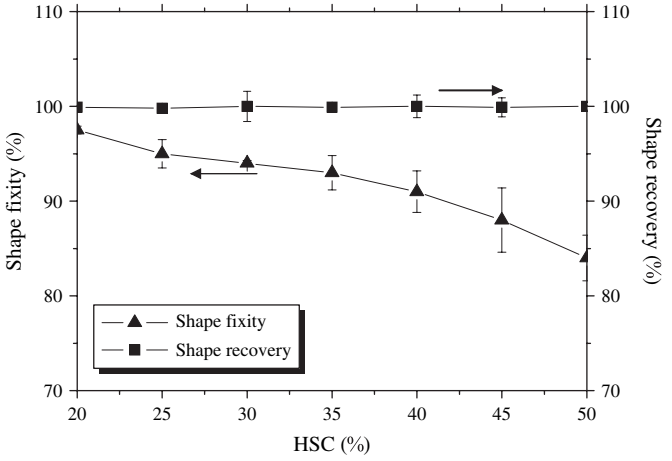

Fig. 17. Shape memory effect after pre-deformation training.

the viscoelastic deformation of hard-segment phase have taken place in the pre-deformation. In the following deformation process, no more irreversible deformation and viscoelastic deformation of hard-segment phase as long as the deformation amplitude did not exceed that of the pre-deformation. Hence the shape recovery was therefore near 100%.

6. Conclusions

A series of segmented polyurethanes showing shape memory effect were synthesized with HSC varying from 10% to 50%. The segmented polyurethanes had crystalline reversible phase for triggering shape memory effect. The morphology and shape memory effect of the polyurethanes were investigated.

The morphology of the segmented polyurethanes was characterized with the combination of multiple techniques including DSC, TMA, SAXS, and so on. In low HSC zone, the polyurethane PU-10 was experimentally proved to be basically homogeneous and has no hard-segment domains. The polyurethanes possessed more or less hard-segment phase when HSC $\geq$ 15%. The hard-segment domains change from isolated states into interconnected states as HSC increased from 40% to 45%. With the increase of HSC, the crystallinity of soft-segment phase decreased. The microdomain morphological structure of the segmented polyurethanes was investigated; interdomain spacing reduced and the number and size of the hard-segment domains rose as HSC increased.

The shape fixity of the segmented polyurethanes decreased with the increase of HSC. The shape fixity was tightly related to the strain-induced crystallization of the soft-segment phase. As for the segmented polyurethanes with lower HSC, deformation amplitude brought little effect to the shape fixity due to their high crystallinity. But for the segmented polyurethanes with 30% $\leq$ HSC $\leq$ 50%, the shape fixity rose dramatically as the deformation amplitude increased from 50% to 100% since the polyurethanes would not develop great strain-induced crystallization under low deformation strain. Further investigations proved that the segmented polyurethanes should be extended at least over 100% strain to obtain better shape fixity.

In addition, stress relaxation could result in the increase of shape fixity and the increasing tendency rose with increase of HSC.

The segmented polyurethane having no hard-segment domains showed over 90% shape recovery in the thermomechanical cyclic tensile tests with 50% deformation amplitude. This implied that the molecular interactions could also play the role of physical cross-links and enable the segmented polyurethane to show shape memory effect under some particular conditions. The segmented polyurethanes having isolated hard-segment domains showed better shape recovery. The shape recovery of segmented polyurethanes decreased dramatically when the hard-segment domains changed from isolated into interconnected state. When they were heated up to a sufficiently high temperature the shape recovery of all the segmented polyurethanes could increase over 90%. In the segmented polyurethanes with higher HSC, it was the deformation of hard-segment phase that resulted in lower shape recovery at $T_m + 20\,^{\circ}C$. Stress relaxation resulted in the decrease of shape recovery at $T_m + 20\,^{\circ}C$. The decrease of shape recovery was more apparent for the segmented polyurethanes with HSC of 15% and 25%. The shape recovery at $T_m + 20\,^{\circ}C$ decreased as the deformation amplitude increased from 50% to 200%. The decrease stopped when deformation amplitude increased to 250%. The shape recovery of the segmented polyurethanes could be enhanced nearly to 100% by a pre-deformation treatment.

Acknowledgements

The authors gratefully acknowledge the financial support of the Project ''High Performance Advanced Materials for Textiles and Apparel'' coded ''GHS/008/04''of the Institute of Textile and Clothing of The Hong Kong Polytechnic University.

References

[1] Tobushi H, Hara H, Yamada E, Hayashi S. Smart Mater Struct 1996;5:483–91.
[2] Lendlein A, Langer R. Science 2002;296:1673–6.
[3] Ding XM, Hu JL, Tao XM. Text Res J 2004;74:39–43.
[4] Lin JR, Chen LW. J Appl Polym Sci 1998;69:1563–74.
[5] Lin JR, Chen LW. J Appl Polym Sci 1998;69:1575–86.
[6] Kim BK, Shin YJ, Cho SM, Jeong HM. J Polym Sci Part B Polym Phys 2000;38:2652–7.
[7] Kim BK, Lee SY. Polymer 1996;37:5781–93.
[8] Li F, Chen Zhu YW, Zhang X, Xu M. Polymer 1998;39:6929–34.
[9] Li F, Zhang X, Hou J, Xu M, Luo X, Ma D, et al. J Appl Polym Sci 1997;64:1511–6.
[10] Ma D, Wang M, Wang M, Zhang X, Luo X. J Appl Polym Sci 1998;69:947–55.
[11] Luo X, Zhang X, Wang M, Ma D, Xu M, Li F. J Appl Polym Sci 1997;64:2433–40.
[12] Wang M, Luo X, Zhang X, Zhu D. Polym Adv Technol 1997;8:136–9.
[13] Lee BS, Chun BC, Chung YC, Sul KI, Cho JW. Macromolecules 2001;34:6431–7.
[14] Liu C, Chun SB, Mather PT, Zheng L, Haley EH, Coughlin EB. Macromolecules 2002;35:9868–74.
[15] Lendlein A, Kelch S. Angew Chem Int Ed 2002;41:2034–57.
[16] Rousseau IA, Mather PT. J Am Chem Soc 2003;125:15300–1.
[17] Guan Y, Cao Y, Peng Y, Xub J, Chen ASC. Chem Commun 2001;1694–5.
[18] Liu G, Ding X, Cao Y, Zheng Z, Peng Y. Macromolecules 2004;37:2228–32.
[19] Takahashi T, Hayashi N, Hayashi S. J Appl Polym Sci 1996;60:1061–9.
[20] Shirai Y, Hayashi S. Mitsubishi Tech Bull 1988;184:1–6.
[21] Hu JL, Ji FL, Wong YW. Polym Int 2005;54:600–5.
[22] Bogart V, John WC, Gibson PE, Cooper SL. J Polym Sci Polym Phys Ed 1983;21:65–95.
[23] Chu B, Gao T, Li Y, Wang J, Desper CR, Catherine AB. Macromolecules 1992;25:5724–9.
[24] Koberstein JT, Galambos AF, Leung LM. Macromolecules 1992; 25:6195–204.
[25] Valenkar S, Cooper SL. Macromolecules 2000;33:382–94.
[26] Ryan AJ, Willkomm WR, Bergstrom TB, Macosko CW, Koberstein JT, Yu CC, et al. Macromolecules 1991;24:2883–9.
[27] Sonnenschein MF, Lysenko Z, Brune DA, Wendt BL, Schrock AK. Polymer 2005;46:10158–66.
[28] Heijkants RGJC, Schwab LW, Calck RV, Groot JH, Pennings AJ, Schouten AJ. Polymer 2005;46:8981–9.
[29] Korley LTJ, Pate BD, Thomas EL, Hammond PT. Polymer 2006; 47:3073–82.
[30] Laity PR, Taylora JE, Wongb SS, Khunkamchoob P, Norrisb K, Cablec M, et al. Polymer 2004;45:7273–91.
[31] Blundell DJ, Eeckhaut G, Fuller W, Mahendrasingam A, Martin C. Polymer 2002;43:5197–207.
[32] Yi J, Boyce MC, Lee GF, Balizer E. Polymer 2006;47:319–29.
[33] Christenson EM, Anderson JM, Hiltner A, Baer E. Polymer 2005; 46:11744–54.
[34] Orthaber D, Bergmann A, Glatter O. J Appl Cryst 2000;33:218–25.
[35] Koberstein JT, Stein RS. J Polym Sci Part B Polym Phys 1983;21: 1439–72.
[36] Garrett JT, Runt J. Macromolecules 2000;33:6353–9.
[37] Tey SJ, Huang WM, Sokolowski WM. Smart Mater Struct 2001;10: 321–5.
[38] Rubinstein M, Colby RH, editors. Polymer physics. Oxford: New York Press; 2003. p. 199–202.